# Analyse pour la LES d'une base de données de simulations directes

Vincent Moureau, Pascale Domingo, Luc Vervisch

# Analyse pour la LES d'une base de données de simulations directes

V. Moureau[a], P. Domingo[a], L. Vervisch[a]

a. *CORIA, CNRS UMR6614, Université et INSA de Rouen, 76801 SAINT-ETIENNE-DU-ROUVRAY, France*

## Résumé :

*Dans ce papier, des simulations numériques directes d'un injecteur aéronautique à swirl sont analysées avec pour objectif de concevoir de nouvelles fermetures pour les simulations aux grandes échelles. Ce brûleur à swirl a un nombre de Reynolds de 40 000 et un nombre de Reynolds turbulent de 1 400. Il est alimenté avec un prémélange pauvre d'air et de méthane à débit constant. La simulation numérique directe est réalisée avec un maillage de 2,6 milliards de tétraèdres et une résolution de 100 microns dans la zone de combustion. L'analyse réalisée porte à la fois sur la modélisation des flux de la variable d'avancement et sur la modélisation de la variance de sous-maille.*

## Abstract :

*A Direct Numerical Simulation database of a realistic swirl burner is analyzed to provide novel Large-Eddy Simulation closures. The swirl burner features a flow Reynolds number of 40,000 and a turbulent Reynolds number of 1,400, and is operated with a lean air/methane mixture at a constant flow rate. The DNS is performed with a 2.6-billion cell unstructured mesh that leads to a resolution of 0.1 mm. The LES analysis is carried out from two angles : modeling of flux terms entering the balance equation for the reaction progress variable, and modeling of the subgrid-scale scalar variance.*

**Mots clefs : Direct Numerical Simulation ; Premixed combustion**

## 1 Background and objectives

Premixed combustion modeling is a challenging task due to the broad range of scales that interact in the flame brush. In Direct Numerical Simulations (DNS), all these scales are resolved, including intermediate radical species that require mesh resolutions around 20 µm under atmospheric conditions for hydrocarbon fuels [10]. In turbulent combustion modes where the flamelet assumption holds, the flame structure may be mapped onto the major species and solving of intermediate radical species is not mandatory for capturing global flame dynamics. DNS may then be performed using tabulated chemistry with coarser mesh resolutions. This methodology was recently applied in a semi-industrial swirl burner operated with a lean mixture of air and methane [13], where the Reynolds number at the swirler exit is approximately 40,000. The database featuring a mesh of 2.6 billion tetrahedra was generated with the YALES2 code developed at CORIA. This database is analyzed through filtering and averaging in order to discriminate and validate existing LES combustion models, and to design a new closure for the subgrid-scale (SGS) variance of scalars.

## 2 Description of the DNS database and flow solver

The chosen configuration is an aeronautical burner investigated experimentally and numerically [12; 18; 14; 7]. YALES2 solves the low-Mach Navier-Stokes equations with a projection method for constant and variable density flows. These equations are discretized with a 4th-order central scheme in space and a 4th-order Runge-Kutta-like scheme in time. The Poisson equation arising in the projection steps

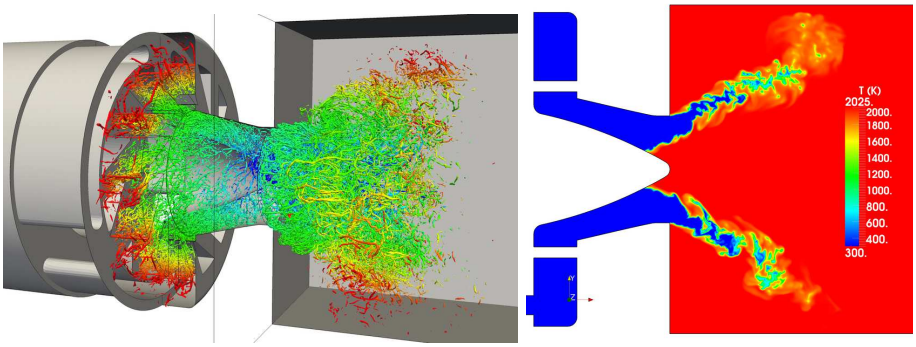


FIGURE 1 – Left : Iso-Q criterion in the swirler and in the combustor (cold-flow simulation). Right : Temperature field in the median plane.

is solved with a highly efficient deflated conjugate gradient. The mesh management of YALES2 allows very large meshes of billions of cells to be handled. It features mesh and solution pre-partitioning and homogeneous mesh refinement based on a non-degenerescent tessellation algorithm for tetrahedrons [17].

In the database, combustion is assumed to be fully premixed, which allows us to model it only through an adequate progress variable. The LES runs are performed with the localized dynamic Smagorinsky model [8] and the PCM-FPI SGS combustion closure [5], whereas the DNS is performed without any model, aside from the premixed flamelet chemistry tabulation.

The DNS features a 2.6-billion-cell unstructured mesh, with a resolution $h_{DNS} = 100\mu$m that is sufficient to resolve most of the turbulent scales, since an approximation of the Kolmogorov scale in the free shear layers developing away from walls, based on the integral length scale and the turbulent Reynolds number, gives an estimate of $\eta = 29$ µm in fresh gases and more than 200 µm in burned gases. The equivalence ratio of the methane/air flame is around 0.83, corresponding to a thermal flame thickness based on the maximum temperature gradient of about 450 µm. Thus, the progress variable profile is resolved with approximately ten points. Figure 1 shows iso-Q criterion surfaces in the cold flow case to illustrate the high intensity of turbulence that is captured in the DNS, along with an instantaneous temperature field for the reactive case evidencing the high level of wrinkling of the flame front.

## 3 Subgrid and diffusive fluxes in the $\tilde{c}$ transport equation

In the transport equation for the Favre-filtered progress variable, $\tilde{c}$, the filtered convective flux, $\overline{\rho \mathbf{u} c}$, is usually decomposed as the sum of a resolved flux, $\overline{\rho}\tilde{\mathbf{u}}\tilde{c}$, and an SGS (or turbulent) flux, $\tau_{sgs} = \overline{\rho \mathbf{u} c} - \overline{\rho}\tilde{\mathbf{u}}\tilde{c}$. A gradient diffusion (GD) assumption is often used to close this subgrid scalar flux :

$$\overline{\rho}\widetilde{u_i c} - \overline{\rho}\tilde{u}_i\tilde{c} = -\frac{\mu_T}{Sc_T}\frac{\partial \tilde{c}}{\partial x_i}\,. \tag{1}$$

The turbulent viscosity, $\mu_T$, is estimated with the same model as that appearing in the unclosed SGS stress, and the SGS Schmidt number, $Sc_T$, is usually fixed to a value smaller than unity. The GD assumption for the subgrid scalar flux has already been challenged in the context of turbulent combustion with RANS (Reynolds Averaging Navier-Stokes), where counter-gradient diffusion has been shown in experiments as well as in DNS [21]. For LES, previous DNS studies [4; 2] have also shown GD and CGD. But contrary to what was observed with RANS, no clear relation with the local intensity of turbulence was found. Moreover, in those DNS, the SGS fluxes were of little consequence compared to the resolved one, suggesting that the error incurred by GD assumption was without much consequence on the LES predictive accuracy. However, these previous DNS were performed with very moderate turbulent Reynolds number (less than 55) and were only two-dimensional. Then, revisiting the SGS scalar flux behavior on the present realistic database with a turbulent Reynolds number of 1,400 will allow those previous observations to be consolidated (or not) and, eventually, will allow construction

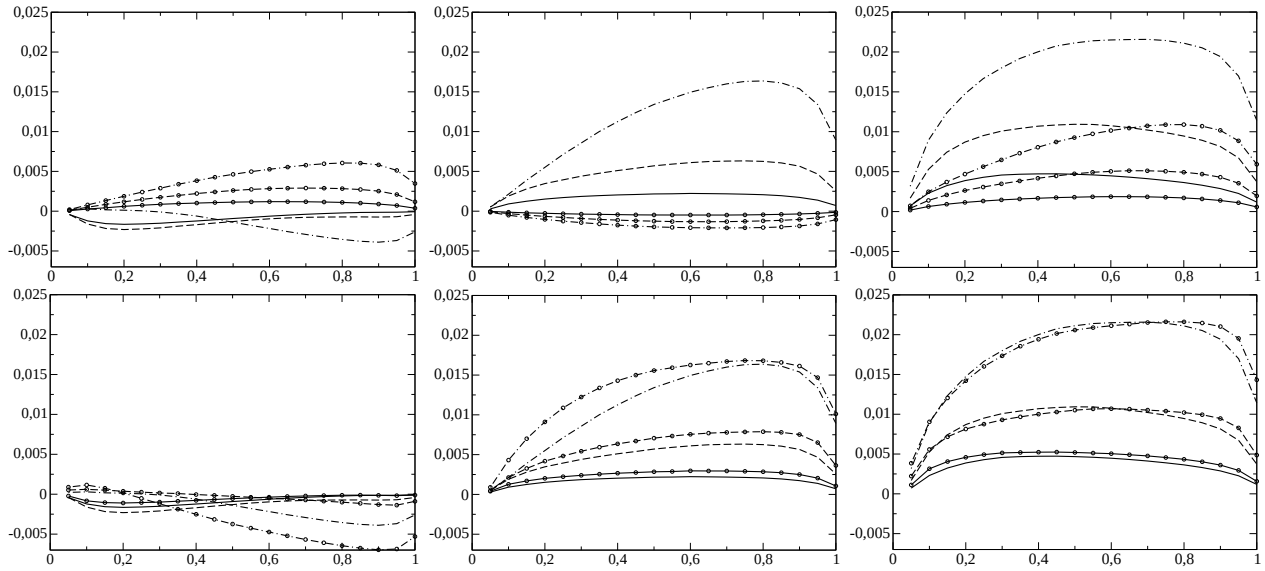

FIGURE 2 – SGS turbulent fluxes versus filtered progress variable : $x$-direction (left), $y$-direction (center), $z$-direction (right). DNS (lines) versus model (lines with symbol). Top : gradient closure ; bottom : scale similarity hypothesis. Filter sizes : continuous line $\Delta = 3h_{DNS}$ ; dashed line : $\Delta = 6h_{DNS}$ ; dot-dashed : $\Delta = 12h_{DNS}$.

of a more accurate closure. Figure 2 (top) presents the evolution of the SGS fluxes in the three spatial directions for various filter sizes. Conditional means on the filtered progress variable are used to present the results. As expected, the SGS flux intensity increases as the filter size is increased. The GD assumption (with $Sc_T = 1$) fails to describe the SGS fluxes in $x$ and $y$ directions, which are of CGD type. To avoid spurious error minimization resulting from conditional averaging over all the flame, only a portion of the flow is considered, explaining the different behavior of $\nabla c$ in $y$ and $z$ directions in this axisymmetrical flame in mean level. The GD assumption is realistic in the $z$-direction, with $Sc_T = 0.5$ providing an acceptable agreement, even though the global profile shape is still not fully captured.

Figure 3 presents the divergence of the exact filtered convective scalar flux (continuous line) compared to the divergence of the subgrid scalar flux (continuous line with symbol). Unlike observations on weakly turbulent DNS [4], here for representative filter sizes, the subgrid flux contribution is as high as 25% of the total flux in this realistic DNS, implying that a reliable closure needs to be provided for the subgrid term. Following the scale similarity approach as originally proposed by [1], the subgrid scalar flux may be written as

$$\widetilde{u_i c} - \tilde{u}_i \tilde{c} = \mathcal{C} \left( \widehat{\tilde{u}_i \tilde{c}} - \hat{\tilde{u}}_i \hat{\tilde{c}} \right) , \tag{2}$$

where $\hat{.}$ represents a filtering operation with a filter test, $\hat{\Delta}$, equal or larger to $\Delta$. The model coefficient $\mathcal{C}$ can either be fixed or determined dynamically as proposed by [19] for the SGS stress tensor. The relation of Eq. 2 is compared to the SGS scalar flux extracted from DNS in the Fig. 2 (bottom) with $\mathcal{C} = 1$ and a filter test $\hat{\Delta} = (4/3)\Delta$. In $x$-direction, the closure performs poorly but the SGS flux is negligible there. Otherwise, the model response stays very close to the exact SGS flux. A dynamic model to determine the parameter $\mathcal{C}$ may help to obtain even better concordance.

Compared to the SGS scalar flux, the filtered diffusive flux appearing in the $\tilde{c}$ transport equation has received less attention in the literature and is usually simply estimated as

$$\overline{\rho \mathcal{D}(T) \frac{\partial c}{\partial x_i}} \sim \overline{\rho} \mathcal{D}(\tilde{T}) \frac{\partial \tilde{c}}{\partial x_i} . \tag{3}$$

Recently, [6] observed that this simple relation was incorrect even in filtered 1D flames. To quantify the difference between the exact and the resolved diffusive flux, a so-called SGS diffusion flux can be

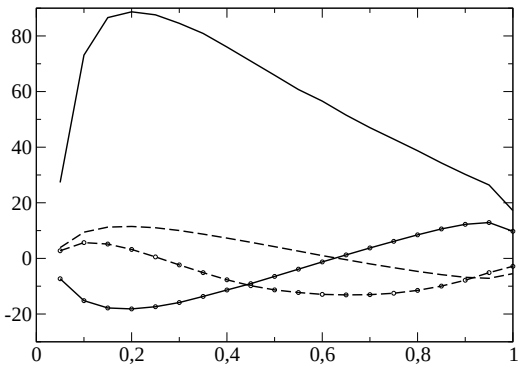


FIGURE 3 – Divergence of the convective and diffusive fluxes vs $\widetilde{c}$ for $\Delta_6$. Continuous line : div $(\overline{\rho \mathbf{u} c})$. Continuous line with symbols : div $(\overline{\rho \mathbf{u} c} - \overline{\rho}\tilde{\mathbf{u}}\tilde{c})$. Dashed line : div $\left(\overline{\rho \mathcal{D} \mathbf{grad} c}\right)$. Dashed line with symbols : div $\left(\overline{\rho \mathcal{D} \mathbf{grad} c} - \overline{\rho}\mathcal{D}(\tilde{T})\mathbf{grad}\tilde{c}\right)$.

introduced :

$$\tau_{sgs,diff} = \overline{\rho \mathcal{D} \frac{\partial c}{\partial x_i}} - \overline{\rho}\mathcal{D}(\tilde{T})\frac{\partial \tilde{c}}{\partial x_i}\,. \tag{4}$$

The divergence of this SGS diffusive flux is plotted in Figure 3 (dashed line with symbol). This term is of the same order as the exact term (dashed line) and is as large as the SGS flux due to convection. Then, neglecting it, as is usually done (Eq. 3), may lead to an inaccurate estimation of the flame propagation speed. The model proposed by [6], which tabulates a correction obtained from a filtered 1D flame, may improve the estimation.

## 4 Scalar variance model description and a priori validation

The SGS scalar energy is one of the basic inputs of turbulent combustion modeling [16], for instance to calibrate the shape of presumed probability density functions used to filter tabulated detailed chemistry [5]. Calculation of the corresponding SGS scalar variances has been the subject of numerous studies and developments [3; 15; 20]. Approaches based on either direct and dynamic estimations of the variance or on its balance equation have been attempted. An alternative is now discussed, grounded on the exact decomposition of the variance into a part computable from the resolved field and an unknown residual contribution.

Any scalar signal $c(\underline{x},t) = \widetilde{c}(\underline{x},t) + c''(\underline{x},t)$ may be decomposed into $\widetilde{c}(\underline{x},t)$, the filtered part that is resolved on the mesh, and $c''(\underline{x},t)$, an unknown SGS part. Following the so-called modified Leonard decomposition, the SGS variance may be cast in $c_v = \widetilde{cc} - \widetilde{c}\widetilde{c} = \mathcal{L}_\phi + \mathcal{M}_\phi$, with a resolved term $\mathcal{L}_\phi = \widetilde{\widetilde{c}\widetilde{c}} - \widetilde{\widetilde{c}}\widetilde{\widetilde{c}}$ and an unknown contribution $\mathcal{M}_\phi = 2(\widetilde{c''\widetilde{c}} - \widetilde{c''}\widetilde{\widetilde{c}}) + \widetilde{c''c''} - \widetilde{c''}\widetilde{c''}$.

In the asymptotic case of a bimodal probability density function of the progress variable $c$, the SGS variance is a simple function of the resolved function $c_v^{\max} = F_v(\widetilde{c}) = \widetilde{c}(1-\widetilde{c})$. It is proposed to adopt this distribution for the modeled part, but to calibrate its amplitude with a parameter $K$ to be determined dynamically : $\mathcal{M}_\phi = K\,F_v(\widetilde{c})$. The modeled variance would then read

$$c_v = \widetilde{\widetilde{c}\widetilde{c}} - \widetilde{\widetilde{c}}\widetilde{\widetilde{c}} + K\,F_v(\widetilde{c})\,. \tag{5}$$

To compute $K$ dynamically according to local flow properties, a test filtering operation denoted $\widehat{\cdot}$ and of size $(4/3)\Delta$ is introduced along with its mass-weighted filtering form $\widetilde{\widetilde{c}}^{*} = \widehat{\overline{\rho}\widetilde{c}}/\widehat{\overline{\rho}}$. Both a usual dynamic procedure (Eq. 6) and the direct application of the model to the scales between filtered and test filtered (Eq. 7) have been attempted to determine $K$. These two options read as

$$\widetilde{\widetilde{c}\widetilde{c}}^{*} - \widetilde{\widetilde{c}}^{*}\widetilde{\widetilde{c}}^{*} = \widetilde{\widetilde{\widetilde{c}}\widetilde{\widetilde{c}}}^{*} - \widetilde{\widetilde{c}}^{*}\widetilde{\widetilde{c}}^{*} + K\left[F_v(\widetilde{\widetilde{c}}^{*}) - \widetilde{F_v(\widetilde{c})}^{*}\right] \tag{6}$$

$$= \widetilde{\widetilde{c}}^{*}\widetilde{\widetilde{c}}^{*} - \widetilde{\widetilde{c}}^{*}\widetilde{\widetilde{c}}^{*} + K\,F_v(\widetilde{\widetilde{c}}^{*})\,, \tag{7}$$

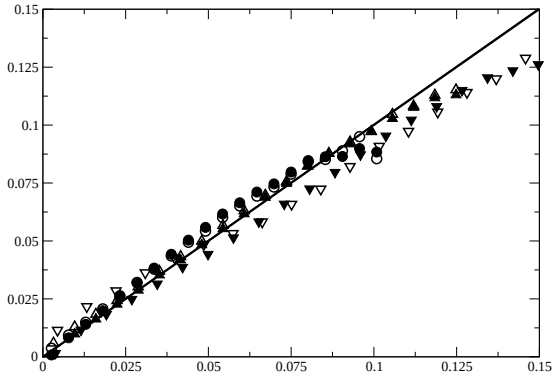


FIGURE 4 – A priori test of Eq. (5), conditional mean of SGS variance versus DNS. Symbols : Eq. (6). Full symbols : Eq. (7). Circle : $\Delta = 4h_{DNS}$ ; triangle-up : $\Delta = 6h_{DNS}$ ; triangle-down : $\Delta = 12h_{DNS}$.

in which all terms are computable, to then determine $K$.

Figure 4 shows the result of *a priori* DNS tests of Eq. (5) combined with Eq. (7) for the dynamic determination of the parameter $K$. Here, $K$ is computed at every flow location within the flame, i.e., where $\widetilde{c}$ is different from zero and unity. The conditional mean of the predicted $c_v$ for the values measured in the DNS is shown in Figure 4 for three typical filter sizes. As expected, when the filter size approaches the integral length scale, high levels of SGS variance are difficult to predict [20], but otherwise the model performs well. In the following, Eq. (7) is retained to compute $K$.

## 5 A posteriori validation of the scalar variance model

*A priori* tests provide a direct assessment of closures in an environment where the relevant variables are known exactly, but those tests obviously suffer from a lack of feedback mechanisms and accumulation of related errors, which must be considered in unsteady simulations [9]. It is therefore essential to proceed with actual LES runs to fully determine the new closure accuracy. To this end, the proposed SGS variance model was implemented in YALES2 during the Summer Program and an LES with a mesh of 14 million tetrahedra ($\Delta/\eta \approx 13$ and $\ell_T/\Delta = 1.77$) was performed using the PCM-FPI closure [5], in which the SGS variance calibrates a filtering operation applied to a premixed laminar flamelet with a beta-presumed probability density function.

The mean and rms $CO_2$ concentration profiles at several locations in the burner are presented in Figure 5. The first conclusion is that Eq. (5) couples well with the iterative solution and preserves its prediction capabilities observed in the *a priori* tests ; the local SGS variance is then dynamically determined according to local flow properties, without resorting to a balance equation and taking advantage of the exact decomposition of the scalar signal. Notice that this experiment is known to have an important 3/4 wave acoustic mode [11], which could explain an increase of all fluctuation levels which is not fully captured by the present LES.

## 6 Summary

Estimations of three-dimensional flame surface from two-dimensional measurements have been tested from DNS of a premixed swirl burner. Then, a dynamic formulation for the filtered burning rate of a progress variable has been validated against the DNS results, also used to probe unresolved SGS diffusive and convective fluxes ; for the latter, a dynamic formulation was discussed. The unresolved part of the molecular diffusive budget, usually neglected in LES, is found of the same order of magnitude as the transport by unresolved velocity fluctuations. Finally, a new dynamic closure was proposed for the SGS variance of scalar and tested in both *a priori* and full LES of the burner.

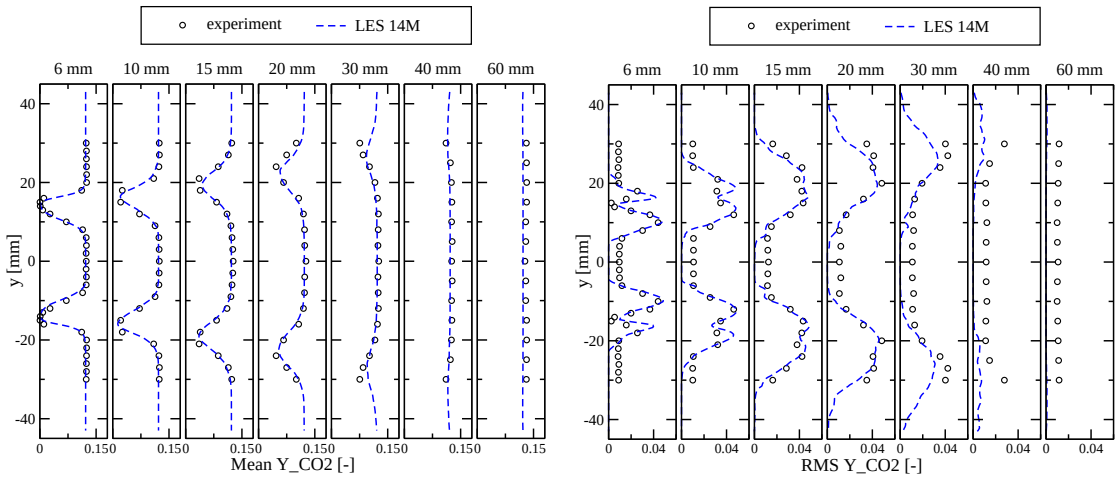


FIGURE 5 – $CO_2$ mass fraction. Left : Mean. Right : Rms. Circle measurement. Dash-line : LES.

# Références


[1] Bardina, J., Ferziger, J. & Reynolds, W. 1984 Improved turbulence models based on les of homogeneous incompressible turbulent flows. *Tech. Rep.* Report TF-19. Stanford Univ., Thermosciences Division, Dept. Mech. Eng.

[2] Boger, M., Veynante, D., Boughanem, H. & Trouvé, A. 1998 Direct numerical simulation analysis of flame surface density concept for large eddy simulation of turbulent premixed combustion. In *Twenty-seventh Symposium (International) on Combustion*, pp. 917 – 925. The Combustion Institute.

[3] Cook, A. W. & Riley, J. J. 1994 A subgrid model for equilibrium chemistry in turbulent flows. *Phys. Fluids* **8** (6), 2868–2870.

[4] Domingo, P., Vervisch, L., Payet, S. & Hauguel, R. 2005 Dns of a premixed turbulent v flame and les of a ducted flame using a fsd-pdf subgrid scale closure with fpi-tabulated chemistry. *Combustion and Flame* **143**, 566–586.

[5] Domingo, P., Vervisch, L. & Veynante, D. 2008 Large-eddy simulation of a lifted methane jet flame in a vitiated coflow. *Combustion and Flame* **152** (3), 415 – 432.

[6] Fiorina, B., Vicquelin, R., Auzillon, P., Darabiha, N., Gicquel, O. & Veynante, D. 2010 A filtered tabulated chemistry model for les of premixed combustion. *Combustion and Flame* **157**, 465–475.

[7] Galpin, J., Naudin, A., Vervisch, L., Angelberger, C., Colin, O. & Domingo, P. 2008 Large-eddy simulation of a fuel-lean premixed turbulent swirl-burner. *Combustion and Flame* **155** (1-2), 247 – 266.

[8] Germano, M., Piomelli, U., Moin, P. & Cabot, W. H. 1991 A dynamic subgrid-scale eddy viscosity model. *Phys. Fluids* **3** (7), 1760–1765.

[9] Geurts, B. J. & Fröhlich, J. 2002 A framework for predicting accuracy limitations in large eddy simulations. *Physics of Fluids* **14** (6), L41–L44.

[10] Hawkes, E. R. & Chen, J. H. 2006 Comparion of direct numerical simulation of lean premixed methane-air flames with strained laminar flame calculations. *Combust. Flame* **144** (1-2), 112–125.

[11] Lartigue, G., Meier, U. & Bérat, C. 2004 Experimental and numerical investigation of self-excited combustion oscillations in a scaled gas turbine combustor. *Applied Thermal Engineering* **24** (11-12), 1583 – 1592.

[12] Meier, W., Weigand, P., Duan, X. & Giezendanner-Thoben, R. 2007 Detailed characterization of the dynamics of thermoacoustic pulsations in a lean premixed swirl flame. *Combustion and Flame* **150** (1-2), 2 – 26.

[13] Moureau, V., Domingo, P. & Vervisch, L. 2010 From large-eddy simulation to direct numerical simulation of a lean premixed swirl flame : Filtered laminar flame-pdf modeling. *In press* .

[14] Moureau, V., Minot, P., Pitsch, H. & Bérat, C. 2007 A ghost-fluid method for large-eddy simulations of premixed combustion in complex geometries. *Journal of Computational Physics* **221** (2), 600 – 614.

[15] Pierce, C. & Moin, P. 1999 A dynamic model for subgrid-scale variance and dissipation rate. *Physics of Fluids* **10** (12), 3041–3044.

[16] Pitsch, H. 2006 Large eddy simulation of turbulent combustion. *Annual Review of Fluid Mechanics* **38**, 453–482.

[17] Rivara, M.-C. 1984 Mesh refinement processes based on the generalized bisection of simplices. *SIAM Journal on Numerical Analysis* **21** (3), 604–613.

[18] Roux, S., Lartigue, G., Poinsot, T., Meier, U. & Berat, C. 2005 Studies of mean and unsteady flow in a swirled combustor using experiments, acoustic analysis, and large eddy simulations. *Comb. Flame* **141** (1-2), 40–54.

[19] Salvetti, M. & Banerjee, S. 1995 A priori tests of a new dynamic subgrid-scale model for finite-difference large-eddy simulations. *Physics of Fluids* **7** (11), 2831–2847.

[20] Vervisch, L., Domingo, P., Lodato, G. & Veynante, D. 2010 Scalar energy fluctuations in large eddy simulation of turbulent flames : statistical budget and mesh quality criterion. *Combustion and Flame* **157** (4), 778–789.

[21] Veynante, D., Trouvé, A., Bray, K. N. C. & Mantel, T. 1997 Gradient and counter-gradient scalar transport in turbulent premixed flames. *J. Fluid Mechs* **332**, 263–293.